While T_c decreases by only 20%, $|dR/dH|$ increases by a factor of 4.

The above results illustrate the distinct magneto-transport in the Sc-substituted pyrochlores. In particular, there is no evidence in the systematics of $\rho(T)$ and $S(T)$ of a polaron mechanism like that shown for the perovskites (*15*). Instead, we propose that the pyrochlores are closer to the Cr spinels (*21*), where large (10^4) decreases in $\rho(T)$ (such as in $CdCr_2Se_4$) have been modeled in terms of a FM-ordering–induced modification of a mobility edge (*22*). The Cr spinels bear more than a superficial resemblance to the pyrochlores: Both are low-*n* systems, both have electronically active A sites, and both exhibit a low-*T* upturn in $\rho(T)$. It would be of interest to extend the theory developed for the Cr spinels to the present case, especially for the purpose of understanding the large MR and its interdependence on T_c.

We have shown that MR near T_c is greatly enhanced in the pyrochlores $Tl_2Mn_2O_7$ with substitution of Sc for Tl, nearly independently of the precise value of T_c. This demonstrates a different paradigm for manipulating MR for magnetic-sensing applications. One of the drawbacks of the perovskites is that the bulk MR can be increased by chemical modification only at the expense of lowering T_c. At present, MR in the pyrochlores only occurs below 200 K, but it may be possible to achieve large MR at room temperature with the use of magnetic ions with larger exchange energies and hence larger values of T_c. Such systems might then be amenable to having their MR increased by chemical substitution as in $Tl_{2-x}Sc_xMn_2O_7$.

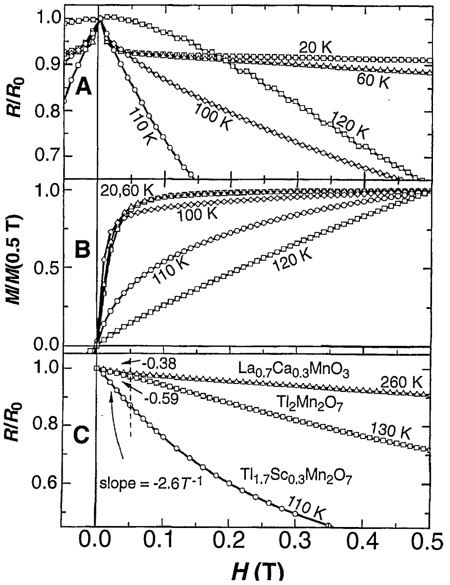

Fig. 4. (**A**) Field dependence of the resistance, normalized to the zero-field value for $Tl_{1.7}Sc_{0.3}Mn_2O_7$ for several temperatures near T_c. Data at small negative field values show an absence of hysteresis. (**B**) Magnetization versus field, normalized to the value at 0.5 T, for various temperatures. (**C**) Normalized resistance versus field for $La_{0.7}Ca_{0.3}MnO_3$, $Tl_2Mn_2O_7$, and $Tl_{1.7}Sc_{0.3}Mn_2O_7$ at the temperature where the intragrain contribution is maximized for each sample.

REFERENCES

1. C. Zener, *Phys. Rev.* **82**, 403 (1951); P.-G. de Gennes, *ibid.* **118**, 141 (1960).
2. A. J. Millis, B. I. Shraiman, R. Mueller, *Phys. Rev. Lett.* **77**, 175 (1996).
3. H. Röder, J. Zhang, A. R. Bishop, *ibid.* **76**, 1356 (1996).
4. Y. Shimikawa, Y. Kubo, T. Manako, *Nature* **379**, 53 (1996).
5. M. A. Subramanian *et al.*, *Science* **273**, 81 (1996).
6. M. E. Fisher and J. S. Langer, *Phys. Rev. Lett.* **20**, 665 (1968).
7. R. M. White and T. H. Geballe, *Long Range Order in Solids* (Academic Press, New York, 1979).
8. D.-K. Seo, M.-H. Whangbo, M. A. Subramanian, *Solid State Commun.* **101**, 417 (1997); D. J. Singh, *Phys. Rev. B* **55**, 313 (1997); S. F. Matar, M. A. Subramanian, J. Etourneau, *J. Mater. Chem.*, in press.
9. S. Jin *et al.*, *Science* **264**, 413 (1994).
10. R. D. Shannon, *Acta Crystallogr.* **32**, 751 (1976).
11. J. E. Greedan, N. P. Raju, M. A. Subramanian, *Solid State Commun.* **99**, 399 (1996).
12. H. Hwang, S-W. Cheong, P. G. Radaelli, M. Marezio, B. Batlogg, *Phys. Rev. Lett.* **75**, 914 (1995).
13. S-W. Cheong, H. Y. Hwang, B. Batlogg, L. W. Rupp Jr., *Solid State Commun.* **98**, 163 (1996).
14. H. J. Fritzsche, *J. Phys. Chem. Solids* **6**, 69 (1958).
15. M. Jaime *et al.*, *Appl. Phys. Lett.* **68**, 1576 (1996).
16. N. F. Mott, *Proc. R. Soc. London Ser. A* **156**, 368 (1936).
17. Y. Tokura, H. Kuwahara, Y. Moritomo, Y. Tomioka, A. Asamitsu, *Phys. Rev. Lett.* **76**, 3184 (1996).
18. K. Khazeni *et al.*, *ibid.*, p. 295.
19. P. Schiffer, A. P. Ramirez, W. Bao, S.-W. Cheong, *ibid.* **75**, 3336 (1995); H. Y. Hwang, S.-W. Cheong, N. P. Ong, B. Batlogg, *ibid.* **77**, 2041 (1996); A. Gupta *et al.*, *Phys. Rev. B* **54**, R15629 (1996).
20. The tunneling contribution in pure $Tl_2Mn_2O_7$ has been studied by H. Hwang and S.-W. Cheong (private communication).
21. A. P. Ramirez, R. J. Cava, J. Krajewski, *Nature* **386**, 156 (1997).
22. E. M. Kogan and M. I. Auslender, *Phys. Status Solidi* **147**, 613 (1988).

23. We would like to acknowledge M. L. Plummer and T. G. Calvarese (both at DuPont) for the high-pressure synthesis experiments and W. J. Marshall (DuPont) for the single-crystal diffractometry data. We acknowledge G. Kotliar, P. Littlewood, P. Majumdar, A. Millis, A. W. Sleight, and H. Y. Hwang for useful discussions and thank A. W. Sleight and P. Majumdar for a critical reading of the manuscript.

5 February 1997; accepted 9 June 1997

Spontaneous Oscillation and Self-Pumped Phase Conjugation in a Photorefractive Polymer Optical Amplifier

A. Grunnet-Jepsen, C. L. Thompson, W. E. Moerner

Optical processing with photorefractive polymers depends on achieving high optical gain, which depends exponentially on the product of the interaction length and the gain coefficient. By use of several polymer layers to increase the overall interaction length and a new high-performance photorefractive polymer composite, the overall optical one-pass gain becomes as large as a factor of 5. For a two-layer sample placed in an optical cavity made with two concave mirrors, spontaneous oscillation due to two-beam coupling gain was observed. Because only one pumping beam is required, this configuration also acts as a self-pumped phase-conjugating mirror with a reflectivity of 13 percent for an applied electric field of 75 volts per micrometer, marking a milestone for this growing class of optoelectronic materials.

The photorefractive (PR) effect refers to optically induced redistribution of charge in an electro-optic material to produce a spatial modulation of the refractive index, or a hologram (*1*). Inorganic crystals showing the PR effect have been known for more than 30 years, and a variety of applications for optical storage and processing have been suggested (*2*). An intriguing new materials class, the PR polymers, are attractive for applications owing to their ease of processing and low cost and, since their inception in 1991 (*3*), many new materials are showing the potential for high performance (*4–6*). The design of a PR polymer requires combining photoconductivity and optical nonlinearity in the same material, and to achieve this, an interdisciplinary combination of synthetic organic chemistry, nonlinear optics, and physical characterization is required (*7*). To illustrate the design strategy, the components of the material used in this study are shown in Fig. 1: (i) Charge (hole) transport is provided by poly(*n*-vinyl carbazole) (PVK); (ii) photoinduced charge generation at red wavelengths is provided by the fullerene C_{60} (*8*); (iii) the electro-optic response is provided by the nonlinear optical chromophore PDCST, which is oriented by an applied electric field; and (iv) lowering of the glass transition temperature

---

Department of Chemistry and Biochemistry, University of California, San Diego, CA 92093–0340, USA.

T_g is provided by the plasticizer BBP. The optical properties of this material, denoted PVK:PDCST:BBP:C_{60}, have been reported recently (9). All PR polymers contain the essential functionalities discussed in (i) to (iii), either as dopants or as moieties covalently attached to a common backbone (*10*).

One optical effect particular to PR materials is two-beam coupling, in which two coherent laser beams intersecting inside the material exchange energy; that is, one beam is amplified and the other is attenuated (Fig. 2A). The sample may be thought of as an optical transistor, in which a pumping beam (the power supply) loses energy while a signal beam (for example, the base current) is amplified by a multiplicative gain factor g upon passage through the sample. This amplification effect relies in an essential way on the nonlocal nature of the index modulation, which is spatially displaced with respect to the optical interference pattern inside the material; such nonlocal gratings are distinctive features of PR materials (*11*). The small signal gain factor g is given by $g = \exp(\Gamma L)$, where L is the interaction length and Γ is the gain coefficient. This exponential growth is similar to that which occurs in a laser material, but in PR polymers there is no stimulated emission, only energy transfer from the pumping beam. Many optical processing applications that rely on large two-beam coupling gain have been proposed and demonstrated, such as machine learning in neural networks, novelty filters, and flip-flops (*12*). Until now, these applications have been restricted to the large gain inorganic PR crystals such as barium titanate. Recently, however, polymer composites with two-beam coupling gain coefficients in the range $\Gamma \sim 200\ \text{cm}^{-1}$ (*4*, *6*, *9*) have been reported (for applied electric fields on the order of 100 V/μm), and these values exceed the largest Γ values for inorganic crystals by an order of magnitude or more. However, the actual gain g has been limited by small sample thicknesses (typically $L = 100$ μm) and by the large electric fields that need to be applied. What is needed for practical applications is $\Gamma L \gg 1$. We now show that by cascading multiple thin-film polymer samples in a simple cavity, the total optical gain can be made to overcome the total optical losses, resulting in spontaneous oscillation (*13*). The configuration may also be regarded as a self-pumped phase-conjugate mirror as described below.

The concept of using layered structures of holographic films to increase the effective material thickness has been suggested previously, first for static holograms (*14*) and recently for PR holograms for storage (*15*). In such stratified volume holographic optical elements, the diffraction efficiency and angular selectivity were strongly dependent on the number of layers, their thickness, and the interlayer spacing. We now show that the same multilayer approach can be adopted to increase the ΓL product during two-beam coupling in a PR material. For this case, the theoretical analysis is even simpler. Two-beam coupling is a cumulative effect, so a signal beam passing through each layer will be amplified by the same factor independent of whether or not any other layers are active (provided there is no pump depletion). In particular, the interlayer spacing is no longer critical.

To demonstrate this principle, we performed two-beam coupling experiments on samples consisting of 140-μm-thick films of the high-performance polymer composite PVK:PDCST:BBP:C_{60} (9) sandwiched between 1.1-mm-thick glass slides coated with indium tin oxide (ITO). Multilayer structures can be easily made by sandwiching several such samples together. In most PR polymers, an applied electric field is essential to assist in charge generation, transport, and establishment of the second-order optical nonlinearity by poling of the chromophores. Figure 2A illustrates the experimental arrangement for a three-layer sample for which a pump (beam 1) and a signal (beam 2) interfere inside the PR polymer structure. All of the layers can be connected to the same power supply to provide the applied external electric field E_o, or the individual layers can be "activated" separately by applying separate voltages. The total gain (symbols) as a function of E_o in one-, two-, and three-layer samples is shown in Fig. 2B. At the highest E_o studied, (single pass) small signal gains as large as a factor of 5 were observed. Fields up to 120 V/μm have been applied to similar samples (9), but because our multilayer sandwich was not carefully designed to avoid electrical breakdown, we chose to use lower fields for this study. The observed increase in gain with the number of layers is in very good agreement with the increase due to a two- and threefold increase in the interaction length; that is, the gain for an N-layer stack of identical samples is $g_N = (g_1)^N$, where g_1 is the single sample gain (*16*, *17*).

A few considerations are relevant when extending the concept to larger stacks. The maximum possible number of layers will ultimately be dictated by the experimental geometry and the need to overlap the interacting beams throughout the whole length. Performance can be improved by increasing the ratio of active to inert material (reducing the thickness of the coated glass slides), and the reflection losses can be reduced by using index-matching gel between the individual samples. Alternatively, one could use glass slides with ITO coating on both sides. This would have the advantage both of eliminating the need for index matching fluid and decreasing the thickness of the sample. For materials with large trap densities in which the counterpropagating geometry is used, the only limit

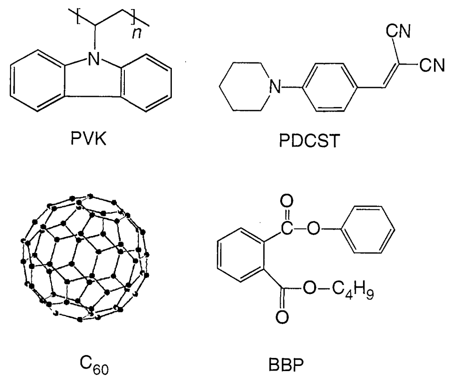

Fig. 1. Sample components: charge-transporting network poly(*n*-vinyl carbazole) (PVK), nonlinear optical chromophore 4-piperidinobenzylidene-malononitrile (PDCST), the fullerene C_{60}, and the liquid plasticizer butyl benzyl phthalate (BBP).

Fig. 2. (**A**) The experimental geometry, which used *p*-polarized 676-nm light from a Kr^+ ion laser. The beam ratio was $\beta = I_1/I_2 = 1000$ and the total intensity $I_o = 250$ mW/cm^2. All layers had a thickness of 140 μm and an absorption coefficient at 676 nm of $\alpha = 8\ \text{cm}^{-1}$. The collimated signal beam was incident at $\theta_2 = 30°$ with a beam diameter of $d_2 = 2$ mm. For the pump beam, $\theta_1 = 60°$ and $d_1 = 5$ mm. (**B**) Two-beam coupling gain in a single sample (□), a two-layer stack (○), and a three-layer stack (▲) of the polymer composite PVK:PDCST:BBP:C_{60}; symbols represent the measured data and the curves a model fit (*16*).

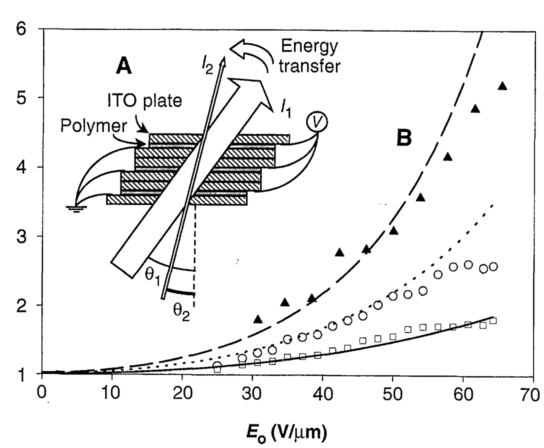

on the thickness of the stack would be the total absorption losses.

With such large optical gains available, we constructed a linear cavity optical resonator (Fig. 3, inset) using two concave mirrors. The principle of operation is based on a single beam (I_1) that is incident on the sample and that will invariably scatter light in various directions (because of impurities and material imperfections). Those weak beams that are scattered in the direction of large gain (here, into smaller angles of incidence) will be amplified due to two-beam coupling. (The direction of energy transfer was previously fixed by the choice of optical polarization and the polarity of the applied electric field.) Of all the amplified scattered light beams, only the beam in the mirror cavity will undergo successive amplification due to optical feedback. Using a two-layer sample and by increasing the gain (by increasing E_o above a threshold of ~45 V/μm), we easily observed the spontaneous formation of a cavity beam by eye on a time scale on the order of seconds. Figure 4 shows an example of the temporal evolution of the transmitted pump beam I_T (dotted line) and the resonator beam I_2 (dashed line, as measured by recording its reflection off the sample) at E_o = 65 V/μm. When the pump beam, I_1, is turned on at t = 1 s, the cavity oscillation as measured by I_2 grows quickly to its steady-state value in about 2 s with a concurrent drop in the intensity of the transmitted signal beam to 10% of its initial value.

A "phase-conjugate" beam, I_4 (Fig. 4, solid line), appears counterpropagating to the incoming pump (Fig. 3, inset), and this beam is delayed slightly from that of the cavity oscillation, but reaches a steady state in about the same time. The physics responsible for the appearance of this beam requires explanation. Optical phase-conjugation has fascinated scientists for almost 50 years (*18*). Popularly referred to as "time reversal," a phase-conjugate (PC) replica of an optical beam will propagate through space with the complex conjugate phase of the original beam, which may be viewed as propagation backward in time. Thus, the PC of an expanding beam, for example, is a focusing beam propagating in the opposite direction, and any distortions of the optical wavefront experienced by the initial beam will be removed when its PC traverses back through the aberrating medium (*19*). The potential applications are many, including the transmission of undistorted images through optical fibers (or the atmosphere), lensless imaging down to submicrometer-size resolution, optical tracking of objects, phase locking of lasers, refreshing of holograms for long-term optical storage, optical interferometry, and image processing (*1*, *2*, *20*).

Phase conjugation is produced when two counterpropagating pump beams intersect in a nonlinear material; a third beam incident will generate its PC replica. The early demonstrations of phase conjugation used a time-consuming process of holographic recording, development, and reading with carefully aligned counterpropagating plane reference waves. Subsequently, dynamic (real-time) phase conjugation was demonstrated with stimulated Brillouin scattering (*21*) and four-wave mixing in a nonlinear optical material (*22*). A major advance was the development of the self-pumped phase conjugator (SPPC) (*23*), which required a PR material. This device does not require a pair of external optical pumps, but instead derives the necessary counterpropagating pump beams directly from the beams I_2 and I_3 in a PR cavity oscillator (Fig. 3, inset). Thus, our PR polymer–based oscillator should automatically act as a SPPC, and the beam I_4 should appear after the cavity oscillation is established (Fig. 4, solid line). The PR polymer sample with its two external mirrors is said to act as a SPPC mirror.

Figure 3 shows the measured PC reflectivity R for a two-layer PR polymer stack, defined by $I_4 = RI_1^*$. As E_o is increased, the two-beam coupling gain increases rapidly until it reaches a threshold value for the onset of cavity oscillation and phase conjugation. Above the threshold, the two-beam coupling gain exceeds the total optical losses of about 40% experienced by the cavity beam for one complete pass. As E_o is increased further, the PC reflectivity increases steadily, reaching a value of 13% at 75 V/μm. This behavior is in good qualitative agreement with the full theory, including the effects of absorption and high modulation depth (*24*). Furthermore, the PC reflectivity is virtually independent of the intensity of the incident beam (open circles and solid triangles), as expected from the standard theory of the PR effect (*9*, *17*). For comparison, reflectivities near 80% have recently been achieved with some inorganic crystals ($BaTiO_3$, $KNbO_3$, and $KTa_{1-x}Nb_xO_3$), with growth times ranging from 10 to 500 s under similar conditions (*2*).

Several considerations underlie the operation of the SPPC. First, the SPPC is self-starting, but with a noticeable delay time governed by the amount of scattering and

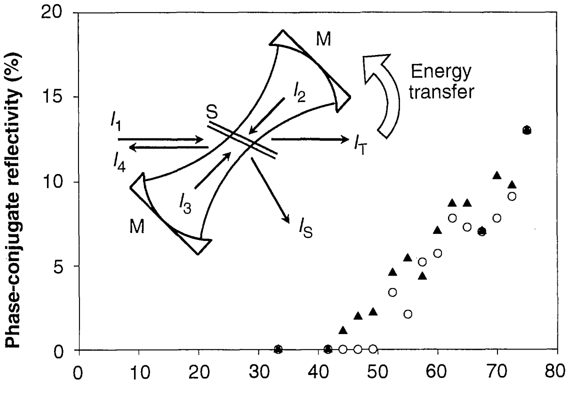

Fig. 3. Self-pumped PC reflectivity R as a function of E_o for a two-layer sample of PVK:PDCST:BBP:C_{60} for an incident intensity of I_1 = 180 mW/cm^2 (▲) and 90 mW/cm^2 (○). No phase conjugation was observed below the threshold of ~45 V/μm. (**Inset**) Experimental arrangement for the linear cavity oscillator. A single pumping beam, I_1, is incident on the sample S at an angle of 50° and is partially reflected, I_S, and transmitted, I_T. When the electric field exceeds a threshold value, the resonator beams, I_2 and I_3, will be set up at an incident angle of 28° between the cavity mirrors (M) spaced 50 cm apart with a radius of curvature of 100 cm. As described in the text, a PC beam I_4 will be generated.

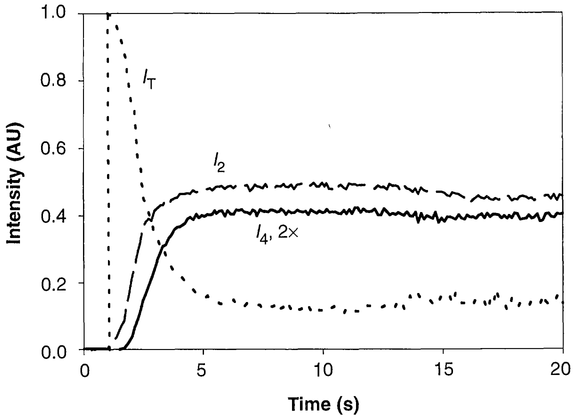

Fig. 4. Temporal evolution of the transmitted beam I_T (dotted line), the resonator beam I_2 (dashed line), and the PC beam I_4 (solid line) for E_o = 65 V/μm and I_1 = 180 mW/cm^2, with the configuration of Fig. 3, inset. I_T and I_4 are normalized to the peak value of I_T, and I_2 is scaled for clarity.

the magnitude of the gain. Thus, the delay time of $\sim$0.5 s observed in Fig. 4 increases to 12 s at $E_o = 46$ V/μm. Furthermore, the use of additional polymer layers will not decrease the threshold for oscillation noticeably unless an index-matching liquid is used to reduce the reflection losses accordingly. Once oscillation has been achieved, however, the PC reflectivity will increase significantly faster with E_o for a larger multilayer stack. Finally, predicting the threshold for oscillation or the value of R from measurements of two-beam coupling gain is not a simple matter. Recent work has shown that these polymers benefit from gain enhancement due to very slow motion of the index grating, which means that the cavity beam is expected to be frequency-shifted from the pumping beam. This complicates the theoretical analysis to a level beyond the scope of this report (*25*).

REFERENCES AND NOTES

1. P. Günter and J.-P. Huignard, Eds., *Photorefractive Materials and Their Applications I & II* (Springer-Verlag, Berlin, 1988 and 1989); P. Yeh, *Introduction to Photorefractive Nonlinear Optics* (Wiley, New York, 1993).
2. L. Solymar, D. J. Webb, A. Grunnet-Jepsen, *The Physics and Applications of Photorefractive Materials* (Oxford Univ. Press, New York, 1996).
3. S. Ducharme, J. C. Scott, R. J. Twieg, W. E. Moerner, *Phys. Rev. Lett.* **66**, 1846 (1991).
4. K. Meerholz, B. L. Volodin, Sandalphon, B. Kippelen, N. Peyghambarian, *Nature* **371**, 497 (1994).
5. M. Liphardt *et al.*, *Science* **263**, 367 (1994); P. M. Lundquist *et al.*, *ibid.* **274**, 1182 (1996); G. P. Wiederrecht, B. A. Yoon, M. R. Wasielewski, *ibid.* **270**, 1794 (1995).
6. W. E. Moerner, A. Grunnet-Jepsen, C. L. Thompson, *Annu. Rev. Mater. Sci.* **27**, 585 (1997).
7. W. E. Moerner and S. M. Silence, *Chem. Rev.* **94**, 127 (1994).
8. S. M. Silence, C. A. Walsh, J. C. Scott, W. E. Moerner, *Appl. Phys. Lett.* **61**, 2967 (1992).
9. A. Grunnet-Jepsen, C. L. Thompson, R. J. Twieg, W. E. Moerner, *ibid.* **70**, 1515 (1997).
10. L. Yu, W. K. Chan, Z. Peng, A. Gharavi, *Acc. Chem. Res.* **29**, 13 (1996).
11. J. P. Huignard and A. Marrakchi, *Opt. Commun.* **38**, 249 (1981).
12. D. Z. Anderson, D. M. Lininger, J. Feinberg, *Opt. Lett.* **12**, 123 (1987); D. M. Lininger, P. J. Martin, D. Z. Anderson, *ibid.* **14**, 697 (1989); D. Z. Anderson, C. Benkert, B. Chorbajian, A. Hermanns, *ibid.* **16**, 250 (1991); A. A. Zozulya, M. Saffman, D. Z. Anderson, *Phys. Rev. Lett.* **73**, 818 (1994).
13. A related effect, beam fanning, has also been observed in our materials and is reported separately (A. Grunnet-Jepsen, C. L. Thompson, R. J. Twieg, W. E. Moerner, *J. Opt. Soc. Am. B*, in press).
14. A. P. Yakimovich, *Opt. Spectrosc.* **49**, 85 (1980); A. R. Tanguay and R. V. Johnson, *J. Opt. Soc. Am. A.* **3**, P53 (1986); G. P. Nordin, R. V. Johnson, A. R. Tanguay, *ibid.* **9**, 2206 (1992).
15. J. J. Stankus, S. M. Silence, W. E. Moerner, G. C. Bjorklund, *Opt. Lett.* **19**, 1480 (1994); R. de Vré and L. Hesselink, *J. Opt. Soc. Am. B.* **11**, 1800 (1994).
16. The theoretical fits were obtained by fitting the standard PR theory (*17*) to the single-layer sample (solid line) as detailed in (*9*) and calculating the gain according to $g_2 = \exp(2\Gamma L)$ (dotted line) and $g_3 = \exp(3\Gamma L)$ (dashed line).
17. N. V. Kukhtarev, V. B. Markov, S. G. Odulov, M. S. Soskin, V. L. Vinetskii, *Ferroelectrics* **22**, 949 (1979).
18. D. Gabor, *Proc. R. Soc. London Ser. A*, **197**, 454 (1949).
19. H. Kogelnik, *Bell Syst. Tech. J.* **44**, 2451 (1965).
20. R. A. Fisher, Ed., *Optical Phase Conjugation* (Academic Press, New York, 1983).
21. B. Ya. Zel'dovich, V. I. Popovichev, V. V. Raguel'sky, F. S. Faizullov, *Sov. Phys. JETP* **15**, 109 (1972).
22. R. W. Hellwarth, *J. Opt. Soc. Am.* **67**, 1 (1977).
23. J. Feinberg and R. W. Hellwarth, *Opt. Lett.* **5**, 519 (1980); J. O. White, M. Cronin-Golomb, B. Fischer, A. Yariv, *Appl. Phys. Lett.* **40**, 450 (1982); J. Feinberg, *Opt. Lett.* **7**, 486 (1982); M. Cronin-Golomb, J. O. White, B. Fischer, A. Yariv, *ibid.*, p. 313; M. Cronin-Golomb, B. Fischer, J. Nilsen, J. O. White, A. Yariv, *Appl. Phys. Lett.* **41**, 219 (1982); M. Cronin-Golomb, B. Fischer, J. O. White, A. Yariv, *ibid.*, p. 689; *IEEE J. Quantum Electron.* **20**, 12 (1984).
24. J. E. Millerd, E. M. Garmire, M. B. Klein, *J. Opt. Soc. Am. B.* **9**, 1499 (1992).
25. V. A. Kalinin and L. Solymar, *Appl. Phys. B.* **45**, 129 (1988).
26. We acknowledge R. J. Twieg for supplying the PDCST chromophore and the U.S. Air Force Office of Scientific Research grant F49620-96-1-0135 for partial support of this work.

20 March 1997; accepted 6 May 1997

Formation of a Silicate L_3 Phase with Continuously Adjustable Pore Sizes

K. M. McGrath, D. M. Dabbs, N. Yao, I. A. Aksay, S. M. Gruner*

The lyotropic L_3 phase was used as a template to form nanoporous monolithic silicates with continuously adjustable pore sizes. The monolith was optically isotropic and transparent with a nonperiodic network. The pore size was adjusted by a change in the solvent volume fraction rather than by a change of the surfactant. Unlike other silicates, the bicontinuous pores were water-filled; removal of surfactant was not necessary to access the pores. Measured characteristic dimensions were from six to more than 35 nanometers. For a given solvent fraction, x-ray scattering indicated little variation of pore widths, in marked contrast to the polydisperse pores of aerogels.

Since the demonstration that surfactants could be used in the fabrication of silica mesophases (*1*), amphiphiles have been used to produce inorganic materials with a variety of mesomorphic structures, including lamellar, hexagonally packed tubular, and cubic forms (*2–12*). Surfactant-induced assembly of inorganic structures is now recognized as a way to make novel nanoporous materials with larger pore sizes than was previously possible. However, techniques developed thus far have limited capability to produce very large pores of a predetermined size. Here we describe the synthesis and characterization of a new, random, bicontinuous silicate mesomorph for which predetermined pore sizes, over a very large size range, may be obtained.

Most procedures for forming mesoporous silicates rely on the micelle-forming properties of a surfactant, typically at a low surfactant concentration. The addition of an inorganic precursor, such as an alkoxysilane, leads to association and coassembly into a mesophase precipitant whose structural dimensions are controlled by the surfactant length. Polymerization of the inorganic precursor and removal of the surfactant results in a rigid silica shell conforming to the structural shape of the mesophase. However, the use of dilute surfactant solutions limits the ability to predict the topology of the mesophase. Also, the typical product of the process is a powder of micrometer-sized particles, thereby limiting uses in filtration, optical, or electronic applications, where large-area thin films or large uniform monoliths of material are required. Finally, the pore volume is filled with surfactant; that is, the surfactant must be removed before the pores can be accessed.

These difficulties may be partially avoided by the use of high-concentration surfactant systems in which either the inorganic precursors minimally perturb a preexisting surfactant-water liquid crystalline (LC) structure or the LC nature of the system may be recovered under appropriate experimental conditions, as shown by Attard *et al.* (*6*). Also, because the inorganic precursor does not precipitate out of solution, the resultant material conforms to the shape of the container in which it forms, thereby allowing fabrication of large monoliths of a desired size and shape. However, even in these cases, the pore size is limited by the surfactant and the limited range of compositions on the phase diagram for a given mesomorphic structure.

Applications of silicate mesophases as filtration media, optical materials, and nanocomposites would be facilitated if the

---

K. M. McGrath and S. M. Gruner, Department of Physics and Princeton Materials Institute, Princeton University, Bowen Hall, 70 Prospect Avenue, Post Office Box 708, Princeton, NJ 08544, USA.
D. M. Dabbs and I. A. Aksay, Department of Chemical Engineering and Princeton Materials Institute, Princeton University, Princeton, NJ 08544, USA.
N. Yao, Princeton Materials Institute, Princeton University, Princeton, NJ 08544, USA.

---

*To whom correspondence should be addressed: Physics Department, Cornell University, Clark Hall, Ithaca, NY 14853–2501.